



Neuroprotective Activities of Long-Acting Granulocyte–Macrophage Colony-Stimulating Factor (mPDM608) in 1-Methyl-4-Phenyl-1,2,3,6-Tetrahydropyridine-Intoxicated Mice

Katherine E. Olson¹ · Krista L. Namminga¹ · Aaron D. Schwab¹ · Mackenzie J. Thurston¹ · Yaman Lu¹ · Ashley Woods² · Lei Lei² · Weijun Shen² · Feng Wang³ · Sean B. Joseph² · Howard E. Gendelman^{1,4} · R. Lee Mosley^{1,4}

Published online: 7 July 2020

© The American Society for Experimental NeuroTherapeutics, Inc. 2020

Abstract

Loss of dopaminergic neurons along the nigrostriatal axis, neuroinflammation, and peripheral immune dysfunction are the pathobiological hallmarks of Parkinson's disease (PD). Granulocyte–macrophage colony-stimulating factor (GM-CSF) has been successfully tested for PD treatment. GM-CSF is a known immune modulator that induces regulatory T cells (Tregs) and serves as a neuronal protectant in a broad range of neurodegenerative diseases. Due to its short half-life, limited biodistribution, and potential adverse effects, alternative long-acting treatment schemes are of immediate need. A long-acting mouse GM-CSF (mPDM608) was developed through Calibr, a Division of Scripps Research. Following mPDM608 treatment, complete hematologic and chemistry profiles and T-cell phenotypes and functions were determined. Neuroprotective and anti-inflammatory capacities of mPDM608 were assessed in 1-methyl-4-phenyl-1,2,3,6-tetrahydropyridine (MPTP)-intoxicated mice that included transcriptomic immune profiles. Treatment with a single dose of mPDM608 resulted in dose-dependent spleen and white blood cell increases with parallel enhancements in Treg numbers and immunosuppressive function. A shift in CD4⁺ T-cell gene expression towards an anti-inflammatory phenotype corresponded with decreased microgliosis and increased dopaminergic neuronal cell survival. mPDM608 elicited a neuroprotective peripheral immune transformation. The observed phenotypic shift and neuroprotective response was greater than observed with recombinant GM-CSF (rGM-CSF) suggesting human PDM608 as a candidate for PD treatment.

Key Words Parkinson's disease · MPTP · neuroprotection · regulatory T cell · Treg · GM-CSF

Electronic supplementary material The online version of this article (<https://doi.org/10.1007/s13311-020-00877-8>) contains supplementary material, which is available to authorized users.

✉ Howard E. Gendelman
hegendel@unmc.edu

✉ R. Lee Mosley
rmosley@unmc.edu

Katherine E. Olson
katherine.olson@unmc.edu

Krista L. Namminga
krista.namminga@unmc.edu

Aaron D. Schwab
aaron.schwab@unmc.edu

Mackenzie J. Thurston
mac.thurston@unmc.edu

Yaman Lu
yaman.lu@unmc.edu

Ashley Woods
awoods@scripps.edu

Lei Lei
leilei@scripps.edu

Weijun Shen
wshen@scripps.edu

Feng Wang
wangfeng@ibp.ac.cn

Sean B. Joseph
sjoseph@scripps.edu

Extended author information available on the last page of the article

Background

Parkinson's disease (PD) is the most common neurodegenerative movement disorder [1] characterized by the loss of dopaminergic neurons along the nigrostriatal axis. Current treatments target disease symptoms [2]. Whereas multiple mechanisms are linked to PD neuropathology, immune dysfunction and neuroinflammation have recently been strongly linked to disease progression and neuronal loss [3–5] and have been observed in both human and animal models of disease [6–11]. Specifically, dysfunctional innate immunity in PD is associated with increased microgliosis, proinflammatory cytokine production, reactive oxygen species levels, and other glial-mediated neurotoxic molecules, all possessing the capacity to influence neuronal cell death [12–16]. Likewise, dysfunctions in the adaptive immune response in PD include decreased CD4⁺ T-cell levels, the presence of effector memory T cells, decreased levels of regulatory T cells (Tregs), and increased frequencies of Th1 and Th17 effector T cells (Teffs) [11, 17–19]. Recent work from our laboratories also indicates that compared to caregiver controls, PD patients' Tregs have limited immunosuppressive function [17, 20]. This dysfunction also correlates with disease status based on Unified Parkinson's Disease Rating Scale (UPDRS) Part III motor assessments. These immune alterations likely contribute to the pathogenesis of disease. Similar adaptive immune aberrations have been observed in amyotrophic lateral sclerosis (ALS), Alzheimer's disease (AD), and Crohn's disease, suggesting a critical role for Tregs in suppressing inflammation [21–23].

Therefore, we hypothesized that increasing Treg number and/or function would be beneficial for PD and other neurodegenerative or neuroinflammatory diseases. This hypothesis led to the exploration of Treg-inducing agents, including vasoactive intestinal peptide (VIP) and granulocyte-macrophage colony-stimulating factor (GM-CSF) [9, 24, 25]. Both immune-modulating agents display potent neuroprotective profiles with beneficial alterations in Treg populations [24, 25]. Specifically, GM-CSF selectively increased Treg frequencies without affecting overall CD4⁺ populations [24]. GM-CSF-induced Tregs also had the capacity to spare dopaminergic neurons within an 1-methyl-4-phenyl-1,2,3,6-tetrahydropyridine (MPTP)-induced lesion. GM-CSF has been linked to neuroprotection in other diseases as well, including AD, traumatic brain injury (TBI), stroke, and myasthenia gravis [26–29]. Many studies have also confirmed its protective capacity is connected to the selective induction of Tregs and/or tolerogenic dendritic cells [24, 27, 30–33].

Clinically, the idea of modifying diseased Treg populations has been tested in both ALS and PD [20, 22]. ALS patients display dysfunctional Tregs that correlate with disease severity and survival [22]. However, if diseased Tregs are isolated and stimulated *ex vivo*, suppressive function is restored,

suggesting a potential therapeutic target. Likewise, direct utilization of human GM-CSF (sargramostim) for the treatment of patients suffering from PD or AD has also displayed promising results [20, 34]. GM-CSF treatment led to modulation of peripheral Treg populations resulting in increased suppressive function in PD patients [20]. This altered immune phenotype decreased motor impairments and improved cortical motor activity. In support, an interim report of the AD study also indicated encouraging results in both activities of daily living and the mini mental state exam (MMSE), suggesting a positive effect on neuronal pathways with GM-CSF treatment [34]. Taken together, these clinical assessments point to the therapeutic benefit of altering the adaptive immune response for the treatment of neurodegenerative disease, and the utilization of GM-CSF to generate that response.

Unfortunately, GM-CSF displays limited bioavailability and a short half-life, requiring the need for higher dosing and daily administration [35–37]. Whereas daily GM-CSF treatment is generally well-tolerated, mild-to-moderate adverse events are also experienced, including injection site reactions, elevation of WBC counts, and bone pain [20, 38, 39]. Therefore, we are investigating strategies to decrease either dose and/or frequency of administration to diminish untoward side effects associated with current dosing regimens. In the current studies and in collaboration with Calibr, we developed and utilized a unique long-acting version of modified recombinant mouse GM-CSF, hereafter denoted as mPDM608. The modification significantly extends the half-life and bioavailability profile of GM-CSF, providing the potential to dose less frequently than recombinant GM-CSF (rGM-CSF) alone. Thus, we tested the ability of long-acting GM-CSF treatment to induce Treg number and/or function and elicit neuroprotective responses similar to or above those previously observed with rGM-CSF administration.

Methods

Animals, mPDM608 Treatment, and MPTP Intoxication

Male, C57BL/6 mice (stock 000664) (6–8 weeks old) were obtained from Jackson Laboratories (Bar Harbor, ME). After acclimation, the mice were injected intraperitoneally (i.p.) with long-acting GM-CSF, mPDM608. For dose-response studies, mice were injected with a single injection at doses ranging from 0 to 30.0 mg/kg. For rGM-CSF protein injections, mice were administered either a single injection (1×) or 5 daily injections (5×) prior to either sacrifice or MPTP intoxication at a dose of 0.1 mg/kg. For neuroprotection experiments, the mice were injected with either vehicle (Dulbecco's phosphate-buffered saline (DPBS), 10 ml/kg body weight) or 1-methyl-4-phenyl-1,2,3,6-

tetrahydropyridine hydrochloride (MPTP-HCl) reconstituted in DPBS obtained from Sigma-Aldrich, St. Louis, MO. The mice received 4 subcutaneous injections of MPTP-HCl (16 mg/kg, MPTP free base), 1 injection at 2-h intervals. MPTP safety precautions were performed in accordance with the MPTP safety and handling protocol [40]. On days 2 and 7 post-MPTP intoxication, mice were sacrificed, and brains were harvested and processed for inflammatory response and neuronal survival, respectively. All of the animals were housed and maintained in accordance with the National Institutes of Health institutional guidelines and approved by the Institutional Animal Care and Use Committee (IACUC) of the University of Nebraska Medical Center.

Perfusions and Immunohistochemistry

While under terminal anesthesia (Fatal Plus, pentobarbital), mice were perfused via cardiac puncture with DPBS followed by 4% paraformaldehyde (Sigma-Aldrich) in DPBS. Following perfusion, whole brains were harvested 7 days post-MPTP and processed to assess dopaminergic neuron survival in the substantia nigra and the striatum. Frozen midbrain sections were cut to 30 μm , immunostained with anti-tyrosine hydroxylase (TH) (anti-TH, 1:2000, EMD Millipore, Burlington, MA), and counterstained for Nissl substance [41]. To assess dopaminergic termini, striatal sections were also labeled with anti-TH (1:1000, EMD Millipore). For labeling of microglia 2 days after MPTP, midbrain sections were immunostained with anti-macrophage antigen complex-1 (Mac-1) (anti-CD11b, 1:1000, AbD Serotech, Oxford, UK). To visualize all antibody-labeled tissues, sections were incubated in streptavidin–horseradish peroxidase (HRP) solution (ABC Elite Vector Kit, Vector Laboratories, Burlingame, CA), color was generated using a glucose oxidase color generation system, and the sections were incubated with diaminobenzidine (DAB) chromogen (ACROS Organics, Fair Lawn, NJ) for visualization. Within the SN, total numbers of Mac-1⁺ cells, TH⁺Nissl⁺ (dopaminergic neurons), and TH⁻Nissl⁺ (nondopaminergic neurons) were enumerated by a blinded investigator and unbiased stereological analysis using Stereo Investigator software under the optical fractionator module (MBF Bioscience, Williston, VT). Densitometry analysis of dopaminergic neuron termini in the striatum was determined using Image J software (National Institutes of Health), as previously described [41].

CD4⁺ T-Cell Isolations

Five days after a single dose of mPDM608 or 5 doses of rGM-CSF administration, donor mice were sacrificed and single-cell suspensions were obtained from spleens. For the genomics study, total CD4⁺ cells were isolated using EasySep Mouse CD4⁺ T Cell Isolation Kit (StemCell, Vancouver,

Canada) per the manufacturer's instructions. For proliferation assays, CD4⁺CD25⁺ Tregs and CD4⁺CD25⁻ conventional responder T cells (Tresps) were isolated from spleen using EasySep Mouse CD4⁺CD25⁺ Regulatory T Cell Isolation Kit II (StemCell) per the manufacturer's instructions. Isolated cell purity was assessed via flow cytometric analysis and was determined to be >90% for all isolations.

Treg Suppression Assays

Cells were isolated as described in the “CD4⁺ T-Cell Isolations” section. The CD4⁺CD25⁺ population served as the Treg population. The CD4⁺CD25⁻ T-cell fraction was collected and pooled from the untreated groups only and served as the Tresp population for the suppression assay. Isolated Tresps were labeled with carboxyfluorescein succinimidyl ester (CFSE) (Thermo Fisher Scientific, Waltham, MA) and plated at a concentration of 5×10^4 in a 96-well U-bottom microtiter plate. Tregs were serially diluted by two-fold dilutions into wells containing Tresps to yield ratios of 1:2, 1:1, 1:0.5, 1:0.25, and 1:0.125 Tresp to Treg, as previously described [17]. The cells were stimulated for proliferation using Dynabeads T-activator CD3/CD28 beads (Thermo Fisher) at a 1:1 bead-to-cell ratio. Stimulated and unstimulated Tresps served as proliferation controls and non-proliferating controls, respectively. Cultures were incubated at 37 °C in 5% CO₂ for 3 days, fixed, and analyzed with a LSRII flow cytometer and FACSDiva Software (BD Biosciences, San Jose, CA).

Flow Cytometric Assessments

Five days after treatment, whole blood and spleens were collected to determine T-cell and B-cell profiles via flow cytometric analysis. Whole blood (50 μl) and splenocytes (1×10^6) were fluorescently labeled using antibodies against extracellular markers for CD3, CD4, CD25, CD8, CD19, and the intracellular marker for FoxP3. Mouse blood and splenocytes were labeled with PerCP-Cy5.5-anti-CD3 (eBioscience, San Diego, CA), PE-Cy7-anti-CD4 (eBioscience), PE-anti-CD25 (eBioscience), FITC-anti-CD8 (eBioscience), and PE-anti-CD19 (eBioscience). For intracellular staining, cells were permeabilized for 45 min at 4 °C using FoxP3/Transcription Factor Staining Buffer Set (eBioscience). The cells were then labeled with APC-anti-FoxP3 (eBioscience) followed by fixation. Samples were analyzed with an LSRII flow cytometer and FACSDiva Software (BD Biosciences). All cell frequencies were determined from the total lymphocyte population.

Blood Chemistry and Peripheral Blood Assessments

At the time of sacrifice, 250 μl whole blood was collected into K₂EDTA blood collection tubes for complete blood

count (CBC) levels or into heparinized blood collection tubes for blood chemistry and metabolite levels. Following isolation, heparinized blood was centrifuged and plasma was collected. Complete metabolic panels were carried out using VetScan Chemistry Comprehensive Test cartridges (Abaxis, Union City, CA) on a VetScan VS2 machine. For CBC analysis, whole blood collected from K₂EDTA tubes was immediately assayed on a VetScan HM5 machine.

RNA Isolation and Transcriptomics

Following CD4⁺ T-cell isolation, total RNA was isolated using the RNeasy Mini Kit (Qiagen, Hilden, Germany) under RNase-free conditions. cDNA was generated from isolated RNA using a RevertAid First Strand cDNA Synthesis kit (Thermo Fisher Scientific), and preamplification was performed using primer mixes for RT² PCR array for Mouse T Helper Cell Differentiation (Qiagen). Quantitative RT-PCR was performed on an Eppendorf Mastercycler Realplex EP (Eppendorf, Hamburg, Germany). Data analysis was completed using RT² Profiler PCR Array web-based data analysis software, version 3.5 (Qiagen) and Ingenuity Pathway Analysis (IPA; Qiagen). Resulting pathways were mapped using only genes significantly upregulated >2-fold. Pathways were arranged and edited for easier visualization using the pathway edit tool in IPA.

Statistical Analyses

All values are expressed as mean ± SEM. Differences in between-group means were analyzed using ANOVA followed by Newman–Keuls *post hoc* test (GraphPad Software, Inc., La Jolla, CA). Comparisons of slope and elevation for CFSE inhibition assays were evaluated using linear regression. Slopes for all lines were significantly nonzero, and linear regression analysis values are expressed on corresponding graphs or noted in the figure legends.

Results

Treatment with mPDM608 Results in Increased Spleen Size, Total Splenocyte Cell Number, and Peripheral Blood Populations

Five days after a single injection of ascending doses of mPDM608, spleens were enlarged (Fig. 1a). Both organ enlargement and increased cell number were dose-dependent ($R^2 = 0.8387$, $p < 0.0001$; $R^2 = 0.7105$, $p < 0.0001$) (Fig. 1b, c). Animals treated with 5 consecutive days of rGM-CSF at doses corresponding to the exact

quantity of GM-CSF within mPDM608 did not experience the same splenomegaly or increased cell number (Fig. 1d–f). In fact, no change was detected with increased dosing of rGM-CSF. Likewise, peripheral blood analysis also indicated a significant increase in number of white blood cells (WBC) and frequency of neutrophils following treatment with mPDM608 (Fig. 1g, h), with a concordant decrease in lymphocyte frequency (Fig. 1i). Monocyte frequencies remained unchanged with treatment, and rGM-CSF treatment did not affect any of these populations (Fig. 1j). However, when observing absolute cell numbers within blood, lymphocytes were not altered with treatment, and a significant increase in monocytes and granulocytes was only observed in 30 mg/kg mPDM608 treatment (Supplemental Fig. 1a–c). Due to the observed spleen enlargement with mPDM608, comprehensive metabolic assessment and peripheral blood analysis were performed to determine any potential toxicities associated with treatment. Significant decreases in albumin and alkaline phosphatase were observed with 1.0 mg/kg, 5.0 mg/kg, 15.0 mg/kg, and 30.0 mg/kg mPDM608 treatment (Supplemental Fig. 2a and b). Alanine aminotransferase, amylase, total bilirubin, urea nitrogen, calcium, phosphorus, creatine, glucose, sodium, and potassium levels remained unchanged with treatment (Supplemental Fig. 2c–2l). rGM-CSF protein treatment did not significantly alter any of these metabolic analytes.

mPDM608 Treatment Significantly Increases CD4⁺CD25⁺FoxP3⁺ Levels in Blood and Spleen and Enhances Immunosuppressive Function

Flow cytometric analysis of lymphocyte populations in peripheral blood revealed that mPDM608 treatment does not affect CD8⁺ levels (Fig. 2a). However, CD4⁺ levels were significantly decreased (Fig. 2b). In contrast, only treatment with 30.0 mg/kg mPDM608 significantly increased CD4⁺CD25⁺FoxP3⁺ cell frequency over control levels (Fig. 2c). Treatment with increased dosing of rGM-CSF did not alter CD8⁺ or CD4⁺ levels (Fig. 2d, e), but did result in a modest rise in CD4⁺CD25⁺FoxP3⁺ levels that was insignificant (Fig. 2f). Flow cytometric analysis of splenic lymphocyte populations following treatment with mPDM608 revealed slightly different results. mPDM608 treatment resulted in a significant decrease in CD8⁺ levels with 3.0 mg/kg, 10.0 mg/kg, and 30.0 mg/kg treatment (Fig. 2g) and no significant changes in CD4⁺ levels (Fig. 2h). A dose-dependent increase in CD4⁺CD25⁺FoxP3⁺ levels was also observed ($R^2 = 0.72$, $p = 0.0337$) (Fig. 2i). Similar to blood observations, rGM-CSF treatment did not alter CD8 or CD4 levels (Fig. 2j, k), but also resulted in a dose-dependent increase in CD4⁺CD25⁺FoxP3⁺ levels ($R^2 = 0.78$, $p = 0.0197$) (Fig. 2l).

Next, after observing an increase in CD4⁺CD25⁺FoxP3⁺ Treg levels, we sought to determine changes in Treg

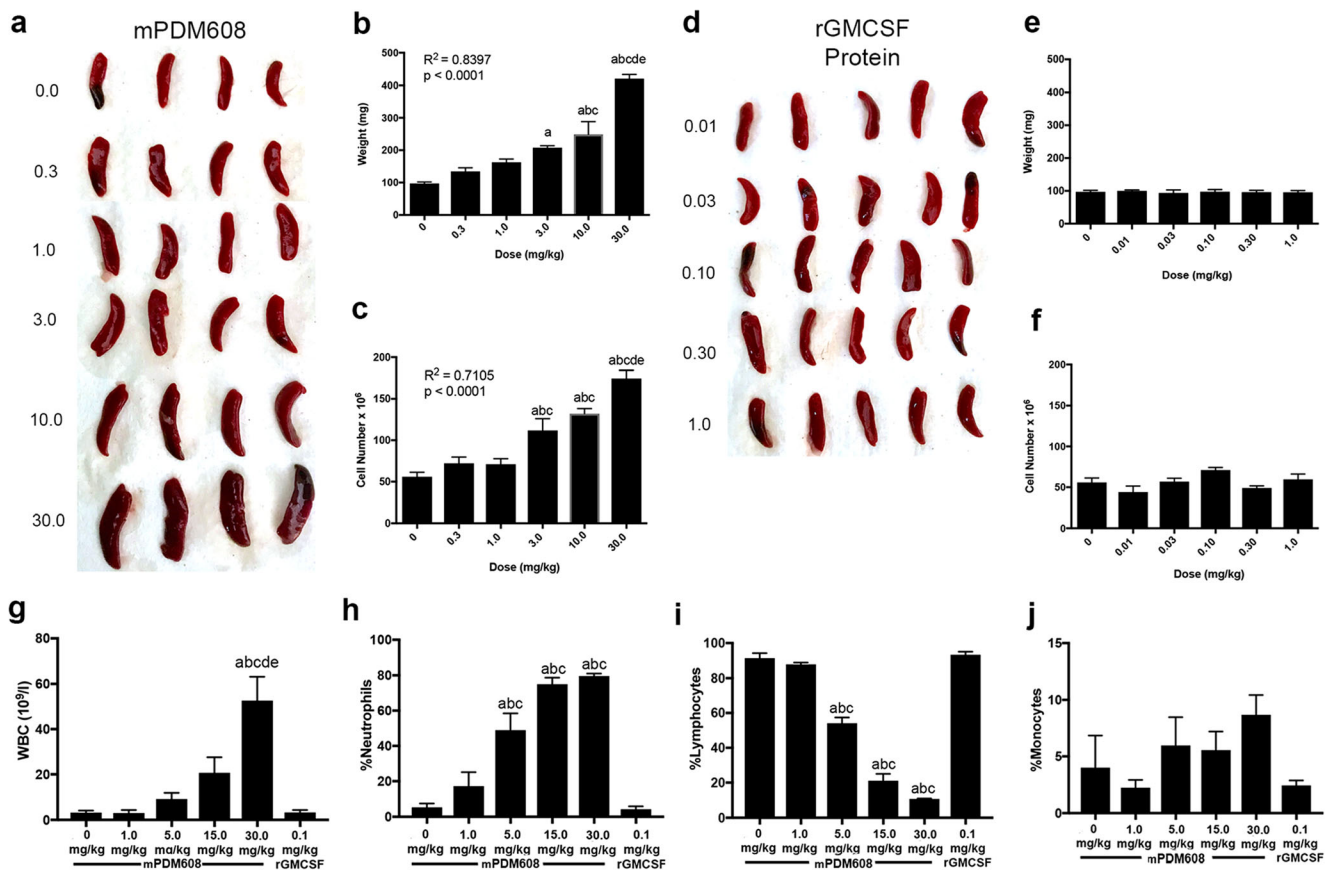


Fig. 1 Treatment with mPDM608 results in dose-dependent splenomegaly and increased peripheral blood cell counts. (a) Visualization of enlarged spleens isolated from mice treated with ascending doses of mPDM608. (b) Quantification of spleen weight 5 days after a single dose of mPDM608 (0–30.0 mg/kg). (c) Total cell number found within the spleen 5 days after a single dose of mPDM608. (b, c) Linear regression analysis located on graphs indicates a dose-dependent response in both organ weight and total cell number following treatment with mPDM608. Significant differences in means (\pm SEM, $n = 5$) were determined by one-way ANOVA and Tukey's *post hoc* test in which $p < 0.05$ compared with treatment of mPDM608 at doses of ^a0 mg/kg, ^b0.3 mg/kg, ^c1.0 mg/kg, ^d3.0 mg/kg,

or ^e10.0 mg/kg. (d) Visualization of spleens isolated from mice treated with ascending doses of rGM-CSF protein. (e) Quantification of spleen weight after 5 consecutive days of treatment with rGM-CSF protein at multiple doses (0.01–1.0 mg/kg). (f) Total cell number quantified within the spleen after 5 consecutive days of treatment with rGM-CSF protein. Complete blood counts were also performed and quantified for percentages of white blood cells (g), neutrophils (h), lymphocytes (i), and monocytes (j) after treatment with various concentrations of mPDM608 or rGM-CSF. Differences in means (\pm SEM, $n = 4$) were determined in which $p < 0.05$ compared with groups treated with ^a0 mg/kg mPDM608, ^b1.0 mg/kg mPDM608, ^crGM-CSF 0.1 mg/kg, ^d5.0 mg/kg mPDM608, or ^e15.0 mg/kg mPDM608

suppressive function utilizing a T-cell proliferation assay. Following treatment with ascending doses of mPDM608 or 0.1 mg/kg rGM-CSF, flow cytometric analysis within splenic populations validated the dose-dependent increase in CD4⁺CD25⁺FoxP3⁺ Treg frequency after treatment with mPDM608 ($R^2 = 0.80$, $p = 0.039$) (Fig. 3a, b). Moreover, dose-dependent increases in Treg frequencies paralleled the increased antiproliferative function (Fig. 3b, c). In fact, significant suppressive function was afforded by Tregs from animals treated with 5.0 mg/kg ($p \leq 0.014$) or 10.0 mg/kg mPDM608 ($p \leq 0.011$) compared to lower doses and untreated controls, thus indicating an enhanced immunosuppressive function (Fig. 3c). Treatment with 10.0 mg/kg mPDM608

resulted in Tregs that demonstrated significantly greater suppressive activity than rGM-CSF-induced Tregs ($p \leq 0.04$).

mPDM608 Pretreatment Attenuates Microgliosis and is Neuroprotective in MPTP-Intoxicated Mice

Following Treg-induction assessments, the ability of mPDM608 treatment to attenuate the neuroinflammatory response associated with MPTP intoxication was assessed by quantifying levels of reactive microglia. Two days post-MPTP intoxication, after pretreatment with mPDM608 or rGM-CSF, ventral midbrains were harvested at a time of peak

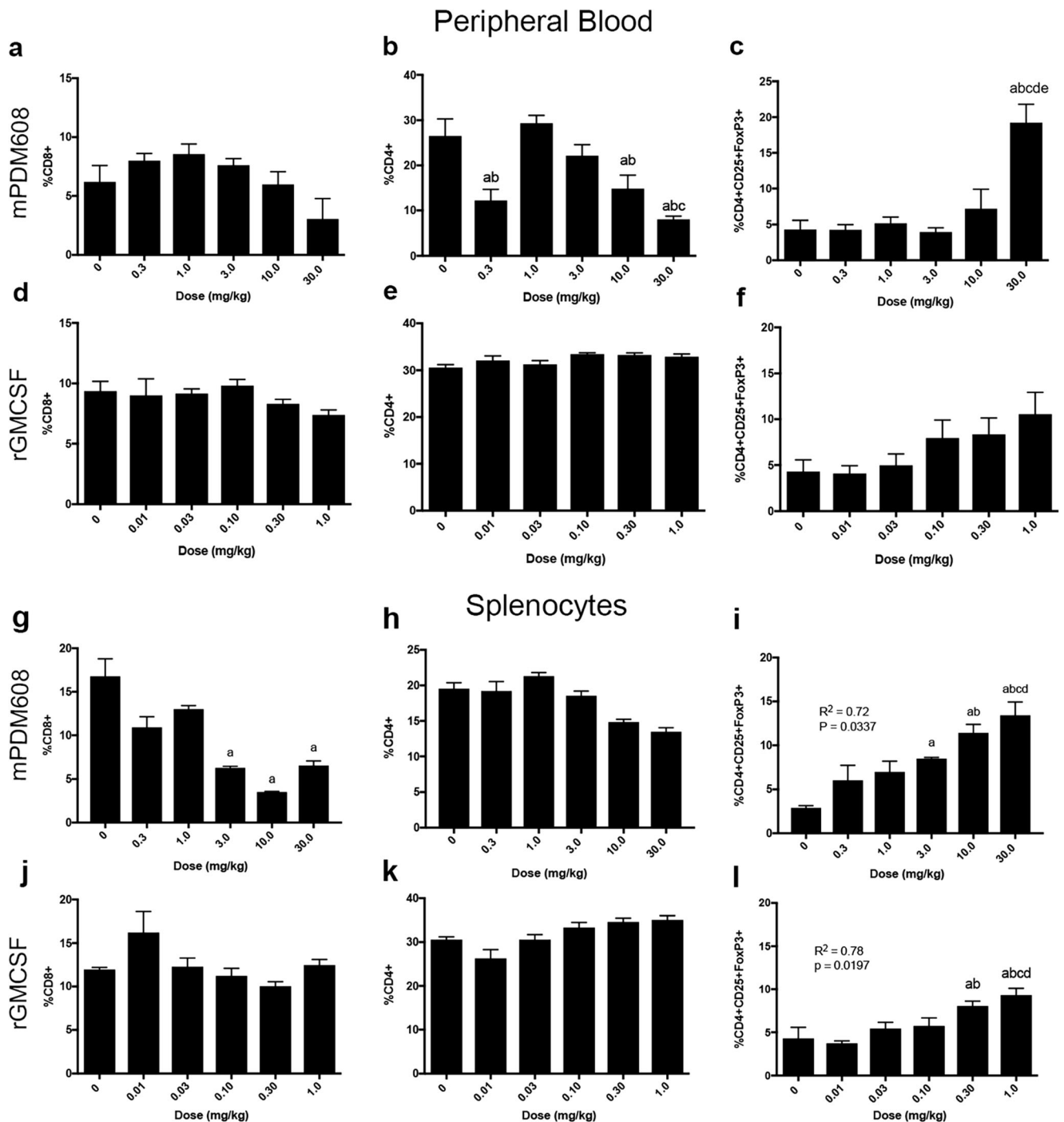


Fig. 2 mPDM608 treatment affects T-cell populations in peripheral blood and spleen. Quantification of CD8⁺ levels (a), CD4⁺ levels (b), and CD4⁺CD25⁺FoxP3⁺ regulatory T-cell (Treg) levels (c) in peripheral blood of mice treated with ascending doses of mPDM608. Differences in means (\pm SEM, $n = 5$) were determined in which $p < 0.05$ compared with ^a0 mg/kg, ^b0.3 mg/kg, ^c1.0 mg/kg, ^d3.0 mg/kg, or ^e10.0 mg/kg treatment. Quantification of CD8⁺ levels (d), CD4⁺ levels (e), and CD4⁺CD25⁺FoxP3⁺ Treg levels (f) in peripheral blood of mice treated with ascending doses of rGM-CSF. Quantification of CD8⁺ levels (g), CD4⁺ levels (h), and CD4⁺CD25⁺FoxP3⁺ Treg levels (i) in spleens isolated from mice treated with ascending doses of mPDM608.

Differences in means (\pm SEM, $n = 5$) were determined in which $p < 0.05$ compared with ^a0 mg/kg treatment, ^b0.3 mg/kg treatment, ^c1.0 mg/kg treatment, and ^d3.0 mg/kg treatment. Quantification of CD8⁺ levels (j), CD4⁺ levels (k), and CD4⁺CD25⁺FoxP3⁺ Treg levels (l) in spleens isolated from mice treated with ascending doses of rGM-CSF. Differences in means (\pm SEM, $n = 5$) were determined in which $p < 0.05$ compared with ^a0 mg/kg, ^b0.01 mg/kg, ^c0.03 mg/kg, or ^d0.10 mg/kg rGM-CSF treatment. Treatment with both mPDM608 and rGM-CSF resulted in a significant dose-dependent increase in Treg levels within the spleen. Linear regression analysis results are provided on graphs (i) and (l)

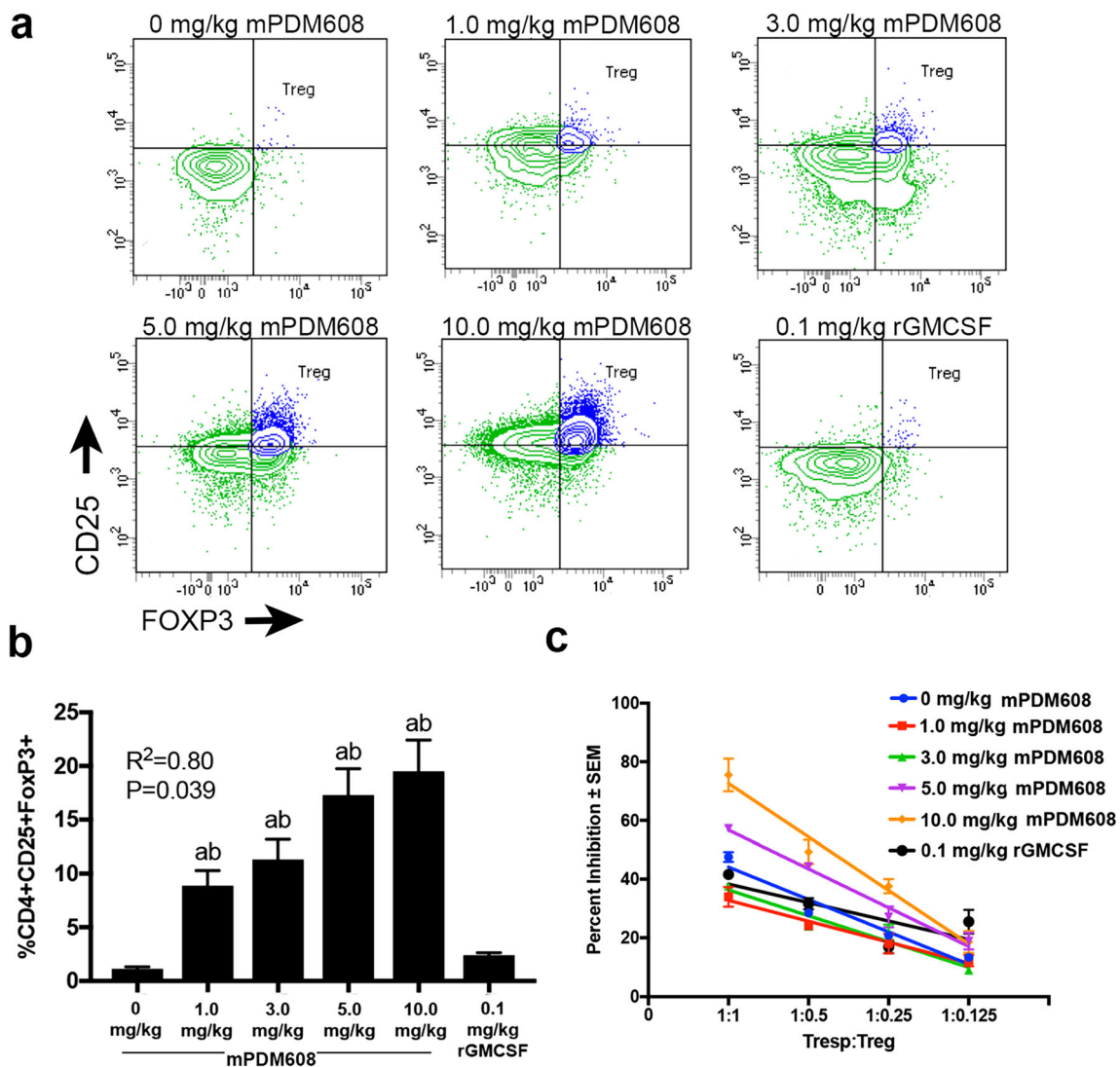


Fig. 3 mPDM608 treatment increases $CD4^+CD25^+FoxP3^+$ Treg levels and cellular function. (a) Representative dual-color histograms of $CD4^+CD25^+FoxP3^+$ Tregs within the gated $CD4^+$ splenic lymphocyte populations from mPDM608- or rGM-CSF-treated mice. The Treg population is indicated by the blue-colored population. (b) Quantification of $CD4^+CD25^+FoxP3^+$ Tregs within spleens following treatment with ascending doses of mPDM608 (0–10.0 mg/kg) or 0.1 mg/kg rGM-CSF. Linear regression analysis of mPDM608 treatment resulted in $R^2=0.80$, $p=0.039$. Differences in means (\pm SEM, $n=5$) were determined in which $p<0.05$ compared with

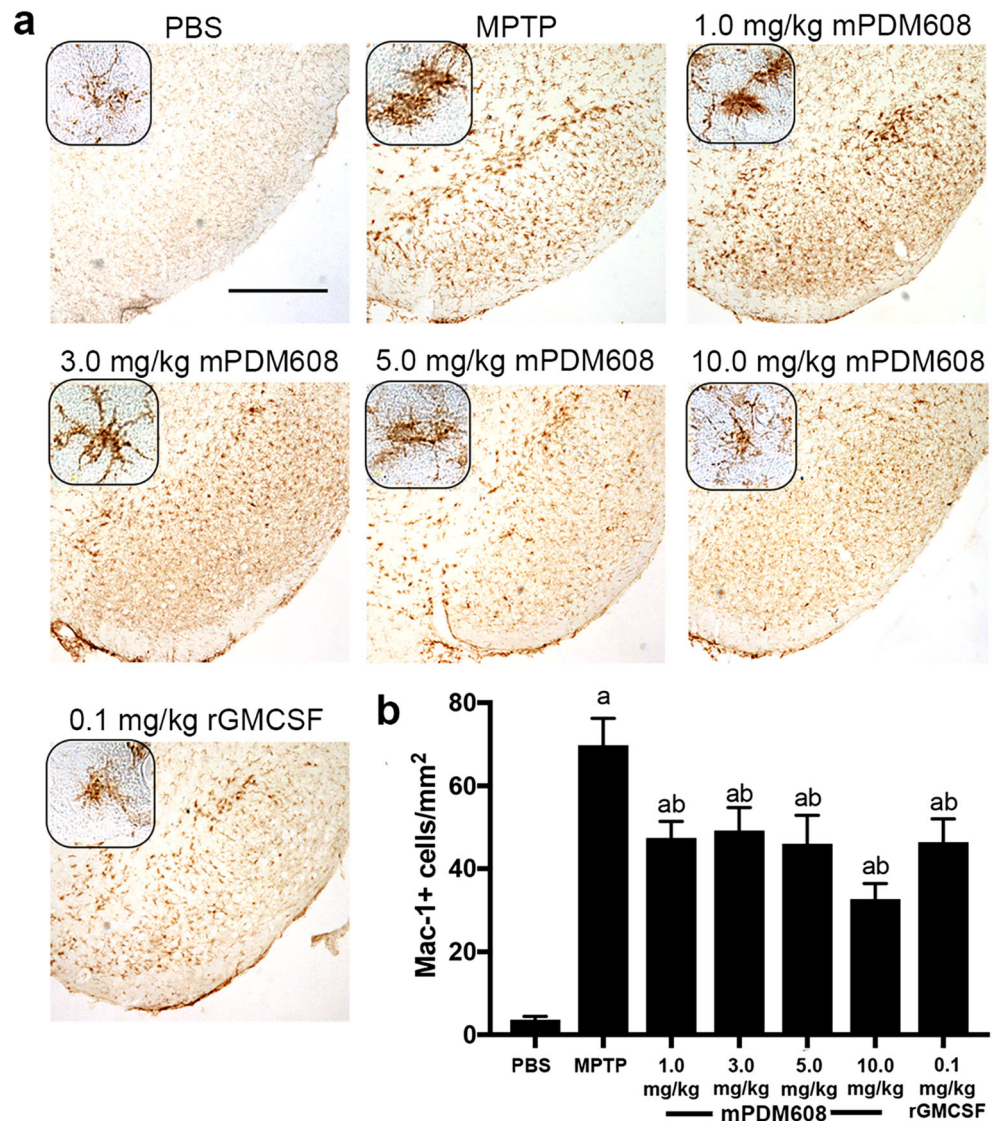
0 mg/kg and rGM-CSF treatment. (c) Quantification of Treg ($CD4^+CD25^+$)-mediated suppression (\pm SEM) of Tresp ($CD4^+CD25^-$) proliferation at various Tresp-to-Treg ratios. Tresp ($CD4^+CD25^-$) were isolated from naïve mice, labeled with CFSE, and stimulated for proliferation for 3 days with anti-CD3/CD28 beads. Treg-mediated suppression is quantified and reported as percent inhibition. Tregs were isolated from untreated (0 mg/kg), mPDM608-treated (1.0–10.0 mg/kg), or rGM-CSF-treated (0.1 mg/kg) mice after 5 days. Linear regression analysis indicates $R^2 \geq 0.93$, $p<0.03$ for all treatments with or without mPDM608; treatment with rGM-CSF resulted in $R^2=0.61$, $p=0.22$

inflammation [6]. Reactivity was assessed by the presence of $Mac-1^+$ microglia with an amoeboid morphology (Fig. 4a). MPTP intoxication significantly elevated reactive microglial counts from 4 ± 0.8 cells/ mm^2 to 70 ± 6.4 cells/ mm^2 compared to PBS controls (Fig. 4b). Treatment with mPDM608 significantly reduced reactive microglia counts to 47 ± 4 cells/ mm^2 for 1.0 mg/kg, 49 ± 5.5 cells/ mm^2 for 3.0 mg/kg, 46 ± 6.8 cells/ mm^2 for 5.0 mg/kg, and 33 ± 3.6 cells/ mm^2 for 10.0 mg/kg compared to MPTP intoxication alone. Treatment with 0.1 mg/kg rGM-CSF also diminished the

neuroinflammatory response by decreasing counts to 46 ± 5.6 cells/ mm^2 .

Due to the observed increase in Treg number and function and decreased inflammatory response, we next tested the neuroprotective capacity of mPDM608 pretreatment in the MPTP mouse model (Fig. 5a). Following MPTP intoxication, dopaminergic neuron numbers dropped significantly from 9313 ± 418 to 4873 ± 211 compared to PBS controls (Fig. 5b). Pretreatment with a single dose of 0.1 mg/kg, 0.3 mg/kg, 1.0 mg/kg, or 3.0 mg/kg mPDM608 provided no significant

Fig. 4 mPDM608 treatment decreases the neuroinflammatory response observed following MPTP intoxication. (a) Immunohistochemistry of Mac-1⁺ microglia in the substantia nigra of mice treated with either PBS, MPTP, 1.0 mg/kg mPDM608, 3.0 mg/kg mPDM608, 5.0 mg/kg mPDM608, 10.0 mg/kg mPDM608, or 0.1 mg/kg rGM-CSF followed by MPTP intoxication ($\times 40$ image; scale bar, 1000 μm ; inset image = $\times 200$). (b) Quantification of reactive microglia within the substantia nigra 2 days post MPTP intoxication. Differences in means (\pm SEM, $n = 5$) were determined in which $p < 0.05$ compared with ^aPBS or ^bMPTP treatment



neuronal survival, resulting in 3891 ± 248 , 3631 ± 364 , 5104 ± 488 , and 5089 ± 378 neurons after treatment. However, treatment with 5.0 mg/kg and 10.0 mg/kg mPDM608 resulted in significant neuroprotection compared to MPTP intoxication alone, resulting in 81% and 76% neuronal sparing, respectively. However, as doses increased from 15.0 to 30.0 mg/kg, neuronal survival diminished, suggesting a maximal dose effect, a dual mechanistic effect, or a bimodal effect. In comparison, treatment with 5 consecutive doses of 0.1 mg/kg rGM-CSF also significantly spared dopaminergic neuron numbers, increasing survival from 45% to 78%, respectively. However, use of a single injection of 0.1 mg/kg rGM-CSF did not result in neuroprotection, indicating the requirement for consecutive dosing when utilizing non-long-acting rGM-CSF. Striatal termini survival was also assessed by immunohistochemistry for TH⁺ termini (Fig. 6a). Digital image analysis indicated that treatment with MPTP significantly diminished striatal termini

density compared to PBS-treated controls (Fig. 6b). Pretreatment with 1.0 mg/kg, 20.0 mg/kg, and 25.0 mg/kg mPDM608 modestly spared striatal termini reductions; however, levels were still significantly lower than those of PBS controls. Treatment with all other doses, including mPDM608 and rGM-CSF, did not protect striatal termini, supporting the notion of increased susceptibility of striatal dopaminergic termini.

Due to the observed increase in Treg numbers and neuroprotective response observed 5 days post mPDM608 injection, we next evaluated the long-acting therapeutic potential of a single injection of mPDM608 (Fig. 7). First, we carried out a time-course assessment of T-cell populations within peripheral blood following treatment with mPDM608. A peak T-cell response was observed 5 days post initial injection (day -10), displaying a significant increase in CD3⁺, CD4⁺, and CD4⁺CD25⁺FoxP3⁺ subsets (Fig. 7a, c, d), along with a

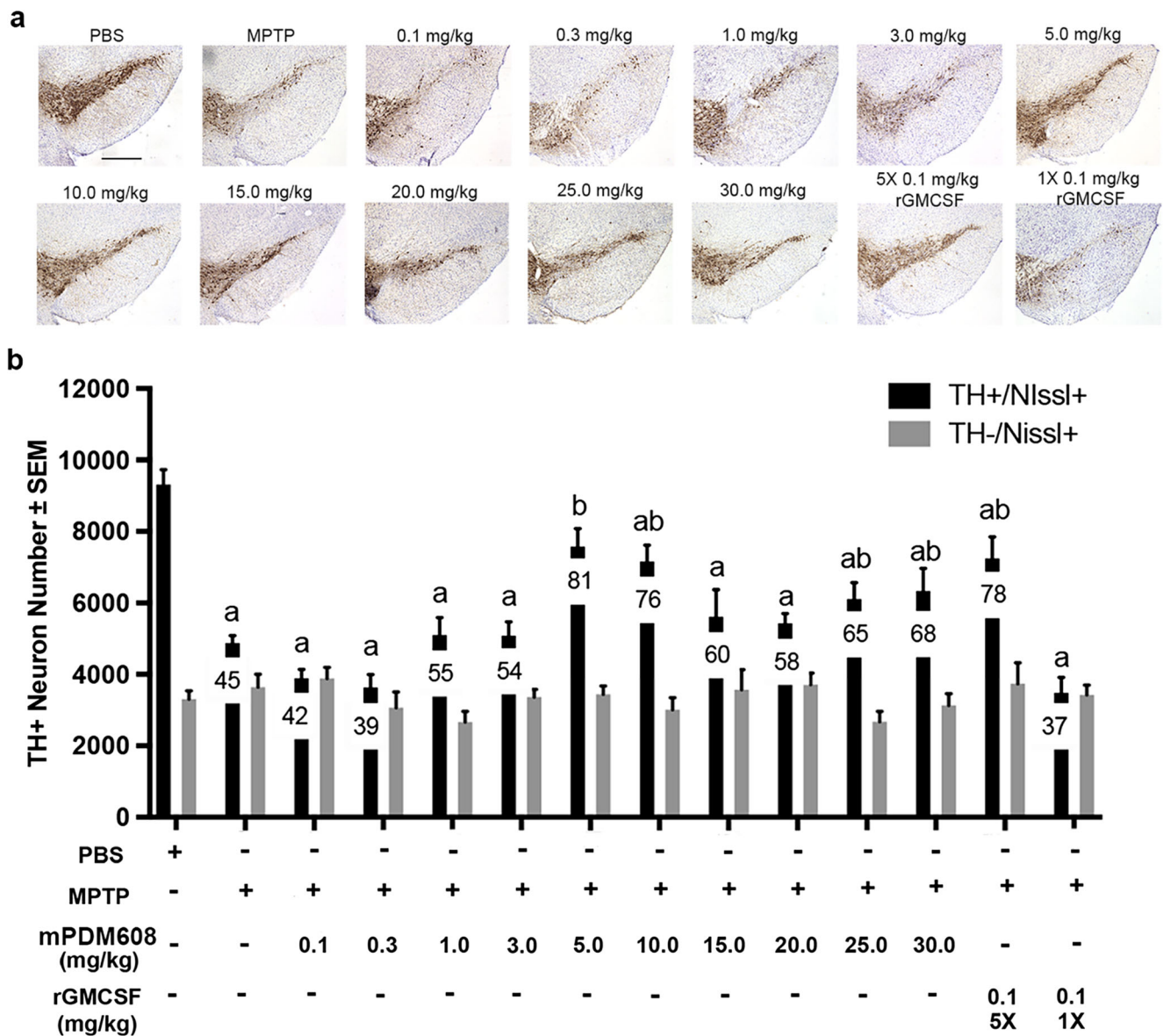


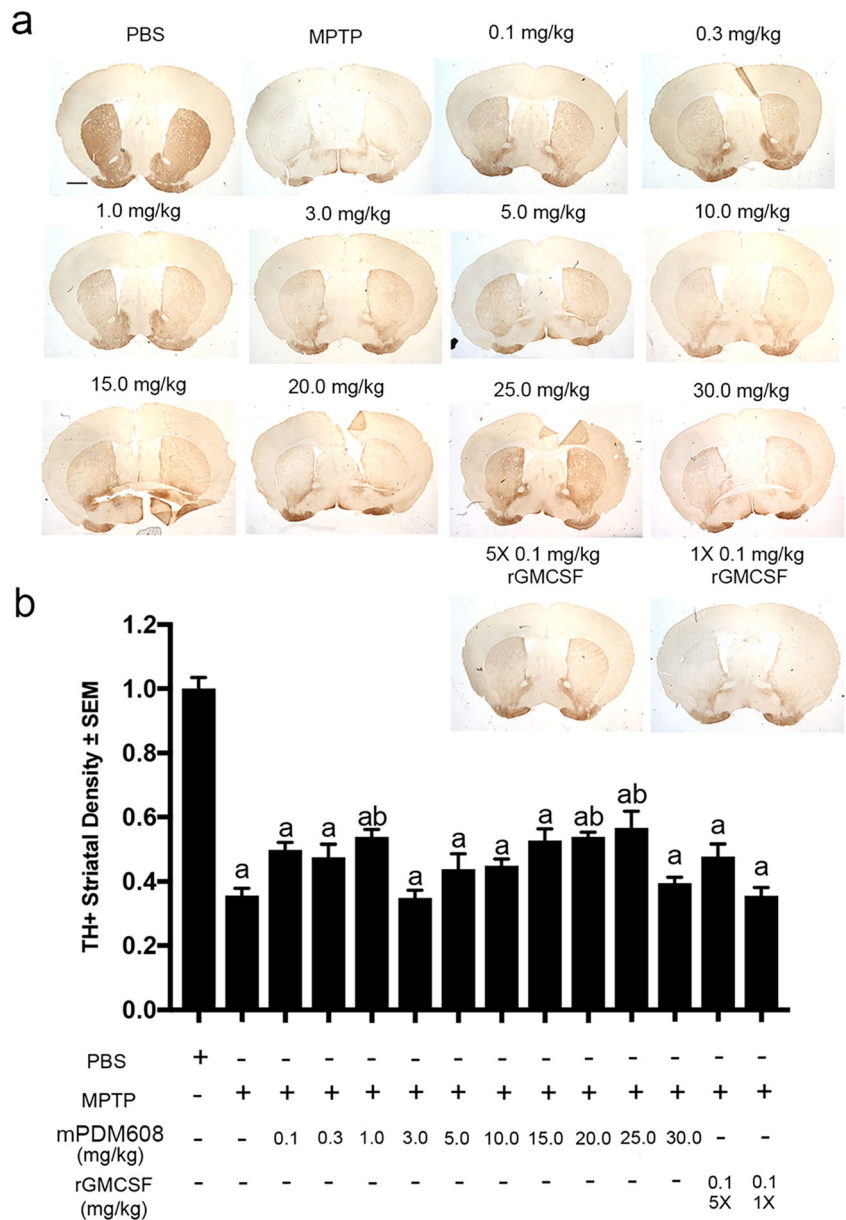
Fig. 5 mPDM608 treatment spares dopaminergic neurons following MPTP intoxication. (a) Representative immunohistochemical sections of TH⁺/Nissl⁺ dopaminergic neurons within the substantia nigra of mice treated with either PBS, MPTP alone, or MPTP and mPDM608 at doses of 0.1, 0.3, 1.0, 3.0, 5.0, 10.0, 15.0, 20.0, 25.0, or 30.0 mg/kg; MPTP and a single injection of 0.1 mg/kg rGM-CSF (1×); or 5 injections (5×) of 0.1 mg/kg rGM-CSF (scale bar = 500 μm). (b) Stereological

quantification of total number of surviving dopaminergic (TH⁺/Nissl⁺) and nondopaminergic (TH⁻/Nissl⁺) neurons within the substantia nigra following MPTP intoxication. Differences in means (± SEM, *n* = 7) were determined in which *p* < 0.05 compared with groups treated with ^aPBS or ^bMPTP. Mean percent remaining total neuron number is indicated on each treatment bar

decrease in the CD8⁺ subset (Fig. 7b). CD3⁺ levels increased from 13.8% ± 0.9 to 21.5% ± 1.1, CD4⁺ levels increased from 8.3% ± 0.6 to 17.7% ± 0.8, and CD4⁺CD25⁺FoxP3⁺ levels increased from 1.8% ± 0.2 to 17.9% ± 2.1, whereas CD8⁺ levels dropped from 5.3% ± 0.3 to 3.5% ± 0.2. Notably, the observed elevations remained significant 10 days post injection (day - 5) but returned to baseline by 14 days post injection (day - 1). Following this treatment paradigm, mice were MPTP

intoxicated and sacrificed 2 days or 7 days post intoxication to assess the inflammatory response and dopaminergic neuron survival, respectively (Fig. 7e, f). MPTP intoxication alone resulted in a significantly increased number of reactive Mac-1⁺ microglia within the ventral midbrain (Fig. 7e). Treatment with mPDM608 15 days prior to MPTP intoxication did not attenuate the observed microgliosis. Treating with mPDM608 10 days or 5 days prior significantly dropped reactive

Fig. 6 mPDM608 treatment attenuates striatal termini loss. (a) Representative immunohistochemical sections of TH⁺ dopaminergic cell termini within the striatum of mice treated with either PBS, MPTP alone, or MPTP and mPDM608 at doses of 0.1, 0.3, 1.0, 3.0, 5.0, 10.0, 15.0, 20.0, 25.0, or 30.0 mg/kg; MPTP and a single injection of 0.1 mg/kg rGM-CSF (1×); or 5 injections (5×) of 0.1 mg/kg rGM-CSF (scale bar = 500 μm). (b) Densitometry analysis of TH⁺ termini within the striatum following MPTP intoxication. Treatment groups are normalized to PBS control density. Differences in means (± SEM, n = 7) were determined in which p < 0.05 compared with groups treated with ^aPBS or ^bMPTP



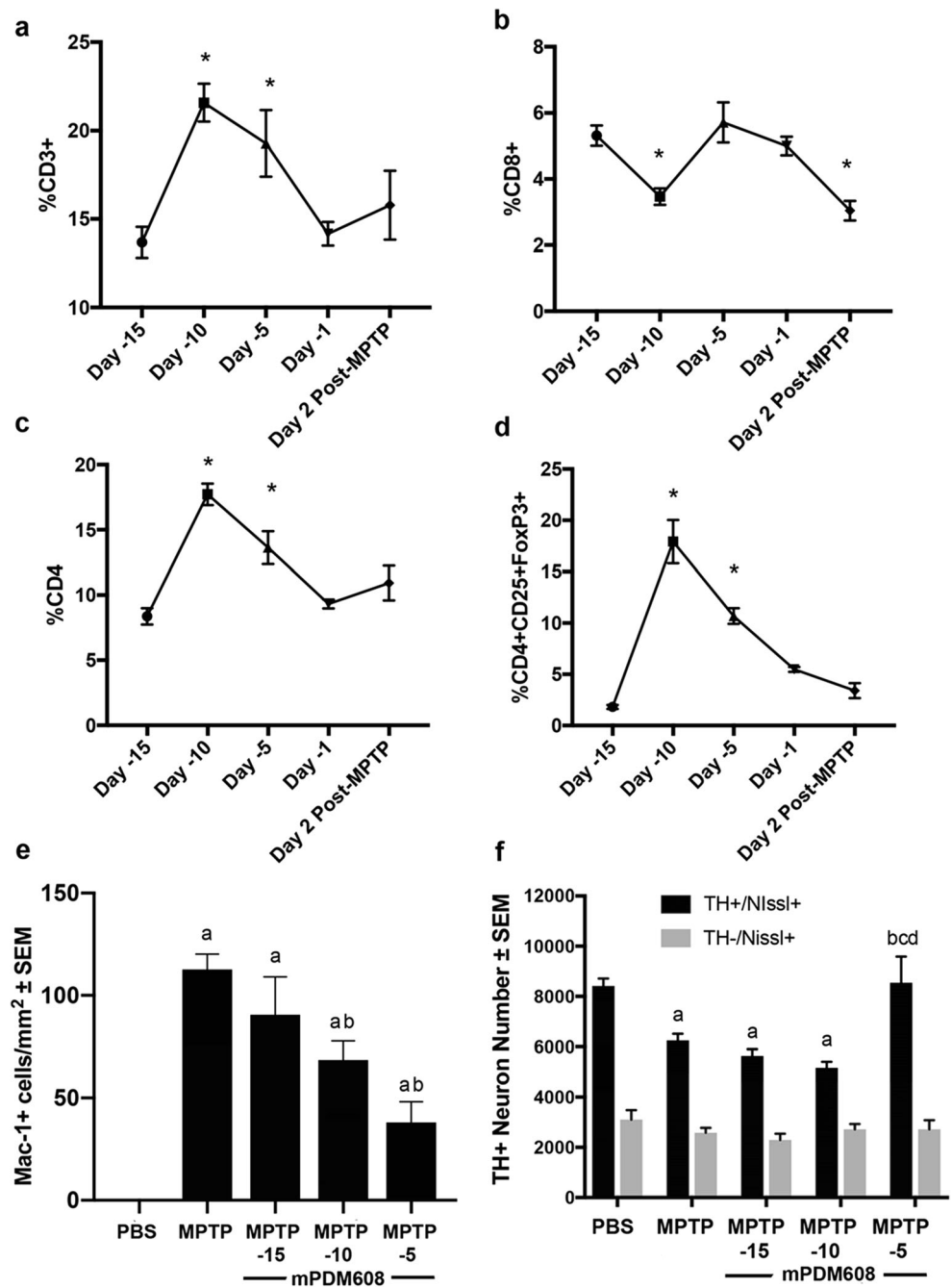
microglial numbers from 113 ± 7 cells/mm² to 69 ± 9 and 38 ± 10 cells/mm². Similarly, MPTP intoxication significantly decreased TH⁺/Nissl⁺ dopaminergic neuron counts from 8418 ± 130 to 6252 ± 292 (Fig. 7f). However, only mPDM608 treatment 5 days prior to MPTP intoxication resulted in significant neuronal sparing, bringing neuron counts back to control levels. Taken together, these findings indicate a potential therapeutic treatment duration up to 10 days.

mPDM608 Treatment Results in an Anti-Inflammatory CD4⁺ T-Cell Phenotype

As peripheral mPDM608 treatment increased Treg frequency and activity, attenuated the neuroinflammatory

response, and selectively mitigated MPTP-induced neurotoxicity [8], we examined the effect of treatment with 10.0 mg/kg mPDM608 on peripheral adaptive immune populations, specifically CD4⁺ T cells. Transcriptomic analysis of CD4⁺ T cells after treatment with mPDM608 resulted in significant dysregulation of numerous genes associated with T-cell differentiation normalized to PBS-treated controls (Fig. 8a). Genes upregulated two- to fivefold included *Ccr4*, *Il1r2*, *Il1r1*, *Ccr6*, *Havcr2*, *Il13*, *Maf*, *Rora*, *FoxP3*, and *Pparg*. Genes upregulated more than fivefold included *Il1rl1* and *Il2*. Genes downregulated two- to fivefold included *Nfatc2*, *Gfi2*, *Id2*, *Stat6*, *Nfatc2ip*, *Rel*, *Socs1*, *Chd7*, *Il12rb2*, *Nr4a1*, *Irf1*, *Tgif1*, *Jak1*, *Ptgd2*, *Fasl*, and

Fig. 7 mPDM608 treatment exhibits long-acting anti-inflammatory and immune-modulating properties. Time-course evaluation of CD3⁺ lymphocytes (a), CD8⁺ lymphocytes (b), CD4⁺ lymphocytes (c), and CD4⁺CD25⁺FoxP3⁺ regulatory T cells (d) within peripheral blood following a single injection of 10 mg/kg mPDM608 followed by MPTP intoxication 15 days later. Differences in means (\pm SEM, $n = 5$) were determined in which $p < 0.05$ compared with baseline (day -15). (e) Quantification of reactive microglia (mac-1⁺) within the substantia nigra 2 days post MPTP intoxication. Differences in means (\pm SEM, $n = 5$) were determined in which $p < 0.05$ compared with ^aPBS or ^bMPTP treatment. (f) Stereological quantification of total number of surviving dopaminergic (TH⁺/Nissl⁺) and nondopaminergic (TH⁻/Nissl⁺) neurons within the substantia nigra 7 days post MPTP intoxication. Differences in means (\pm SEM, $n = 5$) were determined in which $p < 0.05$ compared with groups treated with ^aPBS, ^bMPTP, ^cday -15 mPDM608 + MPTP, and ^dday -10 mPDM608 + MPTP



Il4ra, *Nr4a3* was downregulated more than fivefold. Significantly dysregulated genes were input into Ingenuity Pathway Analysis (IPA) and were shown to be involved in two connecting networks, Hematological System Development and Function, and Inflammatory Response and Cell-Cell Signaling. The two connecting networks were merged using IPA to determine interacting molecules from both pathways (Fig. 8b). As expected, analysis revealed that the main function of the resulting gene alterations predicted changes in the

quantity of lymphocytes and differentiation pathways of induced lymphocytes. In comparison, treatment with 0.1 mg/kg rGM-CSF yielded only minor fold changes in gene expression when normalized to PBS controls (data not shown). Changes in gene expression levels remained below twofold for all genes tested, with the exception of a 2.4-fold upregulation in *Ccr6* and ninefold downregulation in *Tgfr1* levels. However, neither expression level was significantly altered from controls. Therefore, no pathways were assessed for rGM-CSF treatment.

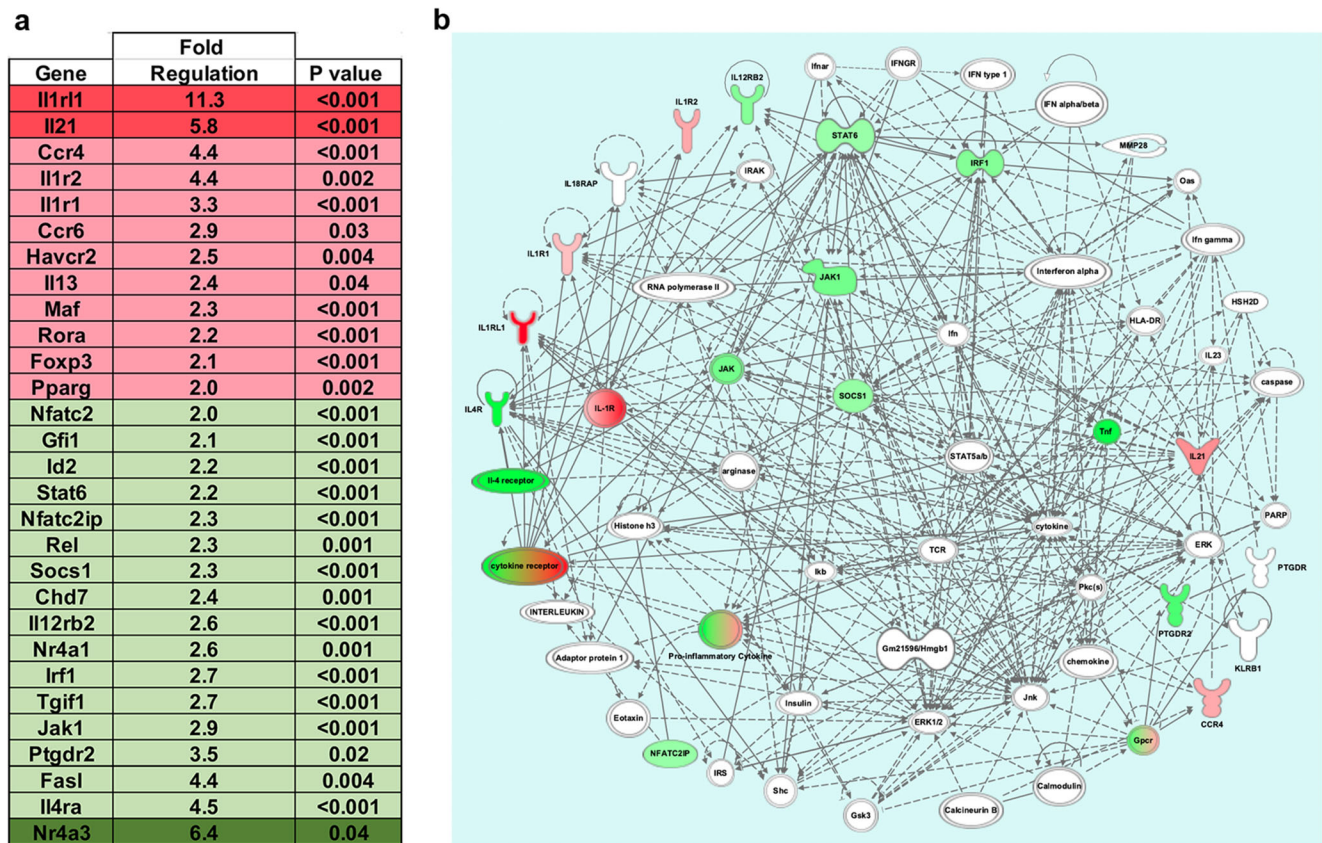


Fig. 8 mPDM608 treatment shifts CD4⁺ T-cell populations into an anti-inflammatory phenotype. Gene expression values from CD4⁺ T cells treated with 10 mg/kg mPDM608 were normalized to PBS treatment. qRT-PCR data show gene expression changes following mPDM608 treatment compared to PBS controls ($n = 4$). Fold changes and p values for differentially regulated gene expression were determined using Qiagen RT² Profiler PCR Array Data Analysis software, version 3.5. Significant differences in fold change were determined in which $p < 0.05$. (a) Table of fold regulation and p values for genes significantly upregulated or downregulated ≥ 2 -fold following treatment with mPDM608. Genes upregulated ≥ 2 - to 5-fold are shown in pink and

> 5 -fold are in red. Genes downregulated ≥ 2 - to 5-fold are shown in light green and > 5 are labeled dark green. (b) Depiction of the direct and indirect network pathways generated using genes from panel (a). The depicted pathway is a merged product of 2 connected networks: hematological system development and function and inflammatory response and cell-to-cell signaling. The resulting gene network was analyzed and prepared using Qiagen's IPA software. Green coloration indicates downregulated genes. Pink or red coloration indicates upregulated genes. Nodes lacking color indicate genes identified by IPA that were not measured but are involved in the signaling pathways. Gray arrows indicate direct relationships between 2 connecting genes

Discussion

GM-CSF treatment has the potential to modify neuroinflammatory diseases based on its known anti-inflammatory capacity and ability to induce Treg populations [20, 24, 27, 30–32, 42]. However, an obstacle for clinical translation is its relatively short half-life and limited bioavailability [36, 37]. Therefore, work presented here characterizes the neuroprotective potential of a long-acting GM-CSF, mPDM608. We hypothesized that treatment with mPDM608 elicits robust Treg induction, anti-inflammatory responses, enhanced neuroprotection, and modulation of peripheral T-cell populations similar to responses previously observed following rGM-CSF treatment [24].

Overall, treatment with mPDM608 was well-tolerated in naïve mice, but did result in a dose-dependent increase in

spleen size, which was an expected pharmacological result [43]. Upon observation of increased spleen size, a toxicity study was carried out and no untoward physical or behavioral side effects were observed including alterations in weight, movement, grooming, and social behavior. Similarly, after 14 days of treatment, spleen sizes returned to normal. The rapid increase in spleen size over the course of 5 days is likely due to the rapid reconstitution and proliferation of immune subsets following therapy as indicated by the increased total cell count within spleens and increased white cell counts within our treatment animals. Similar monocyte and neutrophil alterations were observed in our phase 1 clinical trial but not determined as a serious adverse event [20]. Young rodents are known to experience extramedullary hematopoiesis within the spleen [44]. Although this was not observed with rGM-CSF treatment at the dose levels tested, it is a known side effect of

rGM-CSF treatment in human subjects [43]. Nonetheless, careful monitoring of spleen enlargement following treatment with mPDM608 was carried out parallel to our clinical monitoring in people treated with rGM-CSF. Along with spleen enlargement, treatment with mPDM608 also resulted in a minor decrease in albumin and a more modest decline in alkaline phosphatase levels in plasma. Although significant, decreases in albumin and alkaline phosphatase levels were within normal limits suggesting no malnutrition or adverse health effects from mPDM608 treatment [45, 46].

Treatment with mPDM608 resulted in a dose-dependent increase in Treg numbers that could be sustained up to 10 days after a single injection and also resulted in increased cellular function within the peripheral blood and spleen above those observed with rGM-CSF treatment. rGM-CSF treatment caused a near doubling of Treg numbers although not to a significant level. Previously, we observed a significant increase in Treg numbers following treatment with the same dose of rGM-CSF [24]. The modest variability observed among these 2 studies is likely reflected in the source of rGM-CSF, difference in animals used, investigator variability, and experimental conditions. Nonetheless, mPDM608 significantly increased the number of Tregs induced following treatment, and corresponding elevations following a single injection are also extended for up to 14 days post injection, supporting its long-acting immune-modulating potential. Likewise, Tregs isolated from mPDM608-treated mice displayed increased antiproliferative effects and were able to suppress Tresp proliferation to a greater extent than Tregs isolated from rGM-CSF-treated animals. This increased capacity to suppress immune cell proliferation is likely due to the increased *Maf*, *FoxP3*, *Rora*, and *Pparg* expression levels observed in our transcriptomic studies. *Maf* is a transcription factor that is essential for IL-10 gene expression [47, 48], and IL-10 is an anti-inflammatory cytokine secreted by Tregs to suppress T-cell proliferation via cell cycle arrest [48, 49]. Similarly, both the *FoxP3* and *Rora* transcription factors are important for maintenance of Treg suppressive function [50, 51]. PPAR- γ -expressing Tregs have been shown to control inflammation associated with obesity, and its expression is also a major driver of maintaining Treg phenotype [52, 53]. Therefore, increased mRNA expression likely corresponds to the increased inhibition of T-cell proliferation by mPDM608-induced Tregs observed in functional assays.

rGM-CSF treatment has also been linked to neuroprotection. Our laboratory and others have displayed its potential to increase neuronal survival and decrease microgliosis in models of neurodegenerative disease [20, 24, 26, 28, 54–58]. However, this is achieved through daily dosing. With the long-acting nature of mPDM608, a single-injection scheme achieved a nearly identical level of neuroprotection in the MPTP mouse model. Treatment with mPDM608 significantly spared dopaminergic neuronal cell bodies along with

their projections into the striatum in MPTP-lesioned mice. However, doses greater than 10.0 mg/kg began to decrease the level of neuroprotection observed. This is likely due to the fact that MPTP/MPP+ may be toxic to lymphoid cell populations and may negatively affect proliferating T cells, both Teffs and Tregs, leading to the loss of potentially neuroprotective mPDM608-induced T cells [41]. We have observed this pattern when using other immunomodulating and Treg-inducing agents [25]. Nonetheless, mPDM608 treatment also resulted in a larger anti-inflammatory response than rGM-CSF treatment alone as indicated by decreased microgliosis within the lesion site. The resulting decrease in reactive microglial populations is likely due to the overall anti-inflammatory phenotype in the total CD4⁺ T-cell populations and the increased level of the Treg subset following mPDM608 treatment. Previously, our laboratory indicated the ability of CD4⁺ cells, specifically Tregs, to facilitate microglial phenotype shifts through the regulation of the microglial proteome, suppression of microglial-induced ROS, suppression of NFkB activation, and alterations in mitochondrial function [16, 59, 60].

MPTP intoxication generally results in about 10% neuronal death from the neurotoxin itself [61]. However, for an MPTP-induced lesion to progress and manifest, CD4⁺ T cells are required to maintain the inflammatory microenvironment within the brain [8]. Following MPTP intoxication, CD4⁺ T cells cross the blood–brain barrier (BBB), interact with microglia, shift their phenotype, and enhance production of proinflammatory and neurotoxic mediators [6]. Therefore, the anti-inflammatory phenotype generated through mPDM608 treatment theoretically decreases the level of microgliosis through cell-to-cell interactions and anti-inflammatory cytokine production. Apart from increased IL-10 expression, gene analysis of the CD4⁺ population also indicated profound increases in *il1rl1*, a gene responsible for the ST2 protein, and *IL-13* levels [62]. ST2 is involved in the IL-33 and IL-13 signaling pathway [63]. The IL-33/ST2/IL-13 signaling pathway has been implicated in Treg-dependent suppression in cytomegalovirus infections, Treg-mediated control of inflammation in lung injury, neuroprotection against experimental autoimmune encephalomyelitis (EAE), and immune control in acute graft-versus-host disease (GVHD) [62, 64, 65]. Another study revealed that Tregs expressing the IL-33 receptor, ST2, are highly activated, Th2 biased, and suppress T-cell proliferation through release of IL-10 and TGF β [66]. Thus, this signaling pathway would be a major mechanism in shutting down the inflammatory immune response associated with MPTP lesions, ultimately leading to neuronal survival. A third immune gene that was highly expressed was the *IL-21* gene. IL-21 is a cytokine linked to modulation of Treg homeostasis and maintaining suppressive function in EAE, maintaining immune suppression through IL-10 induction, and reducing proinflammatory cytokine secretion

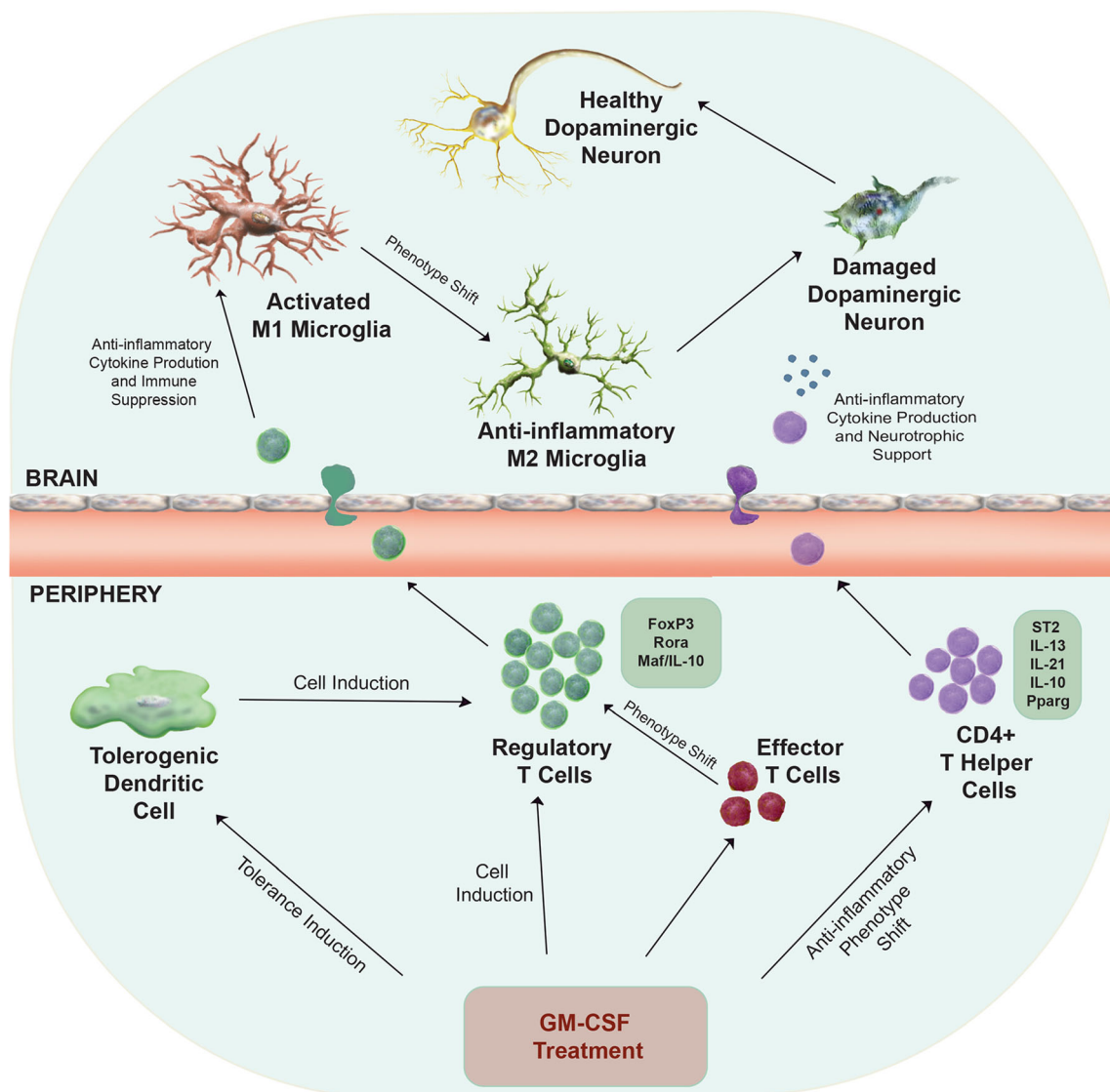


Fig. 9 Proposed immunosuppressive and neuroprotective mechanism of GM-CSF treatment. Neuroinflammation is associated with PD and results in the presence of activated microglia that contribute to an inflammatory microenvironment within the brain. The proinflammatory milieu leads to dopaminergic neuronal cell death. Peripheral administration of GM-CSF leads to neuroprotection and decreased microgliosis through a number of potential immune-mediated mechanisms. Treatment may result in the generation of tolerogenic dendritic cells that can indirectly induce regulatory T-cell populations, direct induction of immunosuppressive regulatory T-cell populations themselves, and/or an anti-inflammatory phenotypic shift in overall CD4⁺ T-cell subsets or effector T-cell

subsets. Specifically, treatment leads to upregulation of genes associated with regulatory T-cell immunosuppressive function, *Foxp3*, *Rora*, and *Maf/IL-10*. Treatment also upregulates genes required for proteins that may be responsible in developing an anti-inflammatory phenotype within the total CD4⁺ T-cell population, including *ST2*, *IL-13*, *IL-21*, *IL-10*, and *Pparg*. Following peripheral immune alterations and cell inductions, regulatory T cells and/or anti-inflammatory CD4⁺ T cells can cross the blood–brain barrier into sites of inflammation and restore the brain’s microenvironment into one that is neurotrophic and anti-inflammatory, leading to increased neuronal survival and health

from activated CD8 cells, all contributing to decrease pro-inflammatory immune responses [67, 68]. In support of an anti-inflammatory phenotype, many of the observed down-regulated genes correspond to genes associated with a pro-inflammatory immune response, such as *Rel/NFkB*, *Nfat*, *IL12rb2*, *irf1*, and *Jak1* [69–72]. *Nr4a3*, the gene found most profoundly decreased, is a gene associated with T-cell proliferation and cell survival [73]. Its reduction may

not have an effect on shifting T-cell phenotype, but on cell survival. Overall, the observed gene changes were associated with an anti-inflammatory response and many genes are directly linked to stabilizing a Treg phenotype. Therefore, we posit that mPDM608 treatment elicits an enhanced neuroprotective and anti-inflammatory profile through either indirect or direct induction of Treg genes associated with maintaining Treg suppression, and genes

resulting in increased anti-inflammatory cytokine production (Fig. 9). These modulations would likely yield a phenotypic shift from proinflammatory M1 microglia into anti-inflammatory M2 microglia leading to overall immune suppression and neurotrophic support within the lesioned brain.

Conclusions

Utilization of our long-acting GM-CSF treatment resulted in an overall immune transformation above that previously observed with standard rGM-CSF treatment. mPDM608 offers the possibility of decreased dosing frequency and increased GM-CSF bioavailability. Treatment with mPDM608 resulted in increased spleen size that corresponded to increased WBC counts, and led to minor shifts in blood chemistry levels. mPDM608 treatment selectively induced Treg populations more than twofold and enhanced Treg immunosuppressive and antiproliferative cellular functions. mPDM608 treatment spared dopaminergic neurons within the SN following MPTP intoxication and decreased the corresponding immune-mediated inflammatory response. The decrease in microgliosis and resulting neuroprotection were linked to the anti-inflammatory and regulatory T-cell phenotype afforded by mPDM608 treatment. Treatment led to increases in Treg-related transcription factors, *maf*, *Rora*, and *FoxP3*, and alterations in genes associated with anti-inflammatory immune responses and cytokine production. Along with its robust neuroprotective and anti-inflammatory profile, all resulting positive changes were achieved using a single dose of mPDM608, rather than consecutive dosing regimens using rGM-CSF, thus supporting the notion that long-acting GM-CSF treatment is translationally appealing and clinically beneficial for the treatment of PD.

Acknowledgments We would like to thank the UNMC Flow Cytometry Research Facility for the exceptional flow cytometric analysis and support. We also thank the INBRE grant from NIH (2P20GM103427) for supporting a site license to EndNote software.

Required Author Forms Disclosure forms provided by the authors are available with the online version of this article.

Availability of Data and Material The datasets used and/or analyzed during the current study are available from the corresponding author upon reasonable request.

Required Author Forms Disclosure forms provided by the authors are available with the online version of this article.

Author Contributions KEO, AW, SBJ, LL, FW, WS, HEG, and RLM designed the experiments. KEO, KLN, YL, MJT, and ADS performed and analyzed the data sets. RLM and KEO performed the statistical analyses. KEO, HEG, AW, SBJ, and RLM interpreted the results. KEO, HEG, and RLM wrote the manuscript. All of the authors reviewed and edited the manuscript and agreed to its contents.

Funding Information The work was supported, in part, by the University of Nebraska Foundation, which includes donations from the Carol Swarts, M.D. Emerging Neuroscience Research Laboratory, the Margaret R. Larson Professorship, and the Frances and Louie Blumkin and Harriet Singer Research Foundations. We thank the Vice Chancellor's Office, of the University of Nebraska Medical Center, for Core Facility support. The research was supported by the California Institute of Biomedical Research (Calibr), Scripps, and National Institutes of Health grants P01 DA028555, R01 NS36126, P01 NS31492, P01 MH64570, P01 NS43985, P30 MH062261, and R01 AG043540 (HEG), and 2R01 NS034239 (HEG and RLM).

Compliance with Ethical Standards

Ethics Approval and Consent to Participate Not applicable.

Consent for Publication Not applicable.

Conflict of Interest The authors from UNMC have no conflict of interest to disclose. AW, SJ, LL, WS, and FW are employees of Calibr, a Division of Scripps Research, which is developing mPDM608 as a clinical candidate.

Abbreviations AD, Alzheimer's disease; ALS, amyotrophic lateral sclerosis; CFSE, 5(6)-carboxyfluorescein N-hydroxysuccinimidyl ester; DAB, 3,3'-diaminobenzidine; DPBS, Dulbecco's phosphate-buffered saline; GM-CSF, granulocyte-macrophage colony-stimulating factor; HRP, horseradish peroxidase; IPA, ingenuity pathway analysis; MPTP, 1-methyl-4-phenyl-1,2,3,6-tetrahydropyridine; PBS, phosphate-buffered saline; PD, Parkinson's disease; rGM-CSF, recombinant granulocyte-macrophage colony-stimulating factor; RT-PCR, reverse transcription polymerase chain reaction; SEM, standard error of the mean; TBI, traumatic brain injury; TH, tyrosine hydroxylase; UPDRS, Unified Parkinson's Disease Rating Scale

References

- Olanow CW, Stern MB, Sethi K: The scientific and clinical basis for the treatment of Parkinson disease (2009). *Neurology* 2009, 72: S1-136.
- Kalia LV, Lang AE: Parkinson's disease. *Lancet* 2015, 386:896-912.
- De Virgilio A, Greco A, Fabbri G et al. Parkinson's disease: autoimmunity and neuroinflammation. *Autoimmun Rev* 2016, 15: 1005-1011.
- Mosley RL, Hutter-Saunders JA, Stone DK, Gendelman HE: Inflammation and adaptive immunity in Parkinson's disease. *Cold Spring Harb Perspect Med* 2012, 2:a009381.
- Anderson KM, Olson KE, Estes KA, Flanagan K, Gendelman HE, Mosley RL: Dual destructive and protective roles of adaptive immunity in neurodegenerative disorders. *Transl Neurodegener* 2014, 3:25.
- Kurkowska-Jastrzebska I, Wronska A, Kohutnicka M, Czlonkowski A, Czlonkowska A: The inflammatory reaction following 1-methyl-4-phenyl-1,2,3,6-tetrahydropyridine intoxication in mouse. *Exp Neurol* 1999, 156:50-61.
- Reynolds AD, Glanzner JG, Kadiu I, et al. Nitrated alpha-synuclein-activated microglial profiling for Parkinson's disease. *J Neurochem* 2008, 104:1504-1525.
- Brochard V, Combadiere B, Prigent A, et al.: Infiltration of CD4+ lymphocytes into the brain contributes to neurodegeneration in a

- mouse model of Parkinson disease. *J Clin Invest* 2009, 119:182-192.
9. Reynolds AD, Stone DK, Hutter JA, Benner EJ, Mosley RL, Gendelman HE: Regulatory T cells attenuate Th17 cell-mediated nigrostriatal dopaminergic neurodegeneration in a model of Parkinson's disease. *J Immunol* 2010, 184:2261-2271.
 10. Iannaccone S, Cerami C, Alessio M, et al. In vivo microglia activation in very early dementia with Lewy bodies, comparison with Parkinson's disease brains. *Parkinsonism Relat Disord* 2013, 19:47-52.
 11. Baba Y, Kuroiwa A, Uitti RJ, Wszolek ZK, Yamada T: Alterations of T-lymphocyte populations in Parkinson disease. *Parkinsonism Relat Disord* 2005, 11:493-498.
 12. McGeer PL, Itagaki S, Boyes BE, McGeer EG: Reactive microglia are positive for HLA-DR in the substantia nigra of Parkinson's and Alzheimer's disease brains. *Neurology* 1988, 38:1285-1291.
 13. Damier P, Hirsch EC, Zhang P, Agid Y, Javoy-Agid F: Glutathione peroxidase, glial cells and Parkinson's disease. *Neuroscience* 1993, 52:1-6.
 14. Chao Y, Wong SC, Tan EK: Evidence of inflammatory system involvement in Parkinson's disease. *Biomed Res Int* 2014, 2014:308654.
 15. Benner EJ, Banerjee R, Reynolds AD, et al. Nitrated alpha-synuclein immunity accelerates degeneration of nigral dopaminergic neurons. *PLoS One* 2008, 3:e1376.
 16. Reynolds AD, Stone DK, Mosley RL, Gendelman HE: Proteomic studies of nitrated alpha-synuclein microglia regulation by CD4+ CD25+ T cells. *J Proteome Res* 2009, 8:3497-3511.
 17. Saunders JA, Estes KA, Kosloski LM, et al.: CD4+ regulatory and effector/memory T-cell subsets profile motor dysfunction in Parkinson's disease. *J Neuroimmune Pharmacol* 2012, 7:927-938.
 18. Kustrimovic N, Comi C, Magistrelli L, et al.: Parkinson's disease patients have a complex phenotypic and functional Th1 bias: cross-sectional studies of CD4+ Th1/Th2/T17 and Treg in drug-naive and drug-treated patients. *J Neuroinflammation* 2018, 15:205.
 19. Bolte AC, Lukens JR: Th17 cells in Parkinson's disease: the bane of the midbrain. *Cell Stem Cell* 2018, 23:5-6.
 20. Gendelman HE, Zhang Y, Santamaria P, et al.: Evaluation of the safety and immunomodulatory effects of sargramostim in a randomized, double-blind phase 1 clinical Parkinson's disease trial. *NPJ Parkinsons Dis* 2017, 3:10.
 21. Yamada A, Arakaki R, Saito M, Tsunematsu T, Kudo Y, Ishimaru N: Role of regulatory T cell in the pathogenesis of inflammatory bowel disease. *World J Gastroenterol* 2016, 22:2195-2205.
 22. Beers DR, Zhao W, Wang J, et al. ALS patients' regulatory T lymphocytes are dysfunctional, and correlate with disease progression rate and severity. *JCI Insight* 2017, 2:e89530.
 23. Pellicano M, Larbi A, Goldeck D, et al: Immune profiling of Alzheimer patients. *J Neuroimmunol* 2012, 242:52-59.
 24. Kosloski LM, Kosmacek EA, Olson KE, Mosley RL, Gendelman HE: GM-CSF induces neuroprotective and anti-inflammatory responses in 1-methyl-4-phenyl-1,2,3,6-tetrahydropyridine intoxicated mice. *J Neuroimmunol* 2013, 265:1-10.
 25. Olson KE, Kosloski-Bilek LM, Anderson KM, et al. Selective VIP receptor agonists facilitate immune transformation for dopaminergic neuroprotection in MPTP-intoxicated mice. *J Neurosci* 2015, 35:16463-16478.
 26. Kiyota T, Machhi J, Lu Y, et al. Granulocyte-macrophage colony-stimulating factor neuroprotective activities in Alzheimer's disease mice. *J Neuroimmunol* 2018, 319:80-92.
 27. Sheng JR, Li LC, Ganesh BB, Prabhakar BS, Meriggioli MN: Regulatory T cells induced by GM-CSF suppress ongoing experimental myasthenia gravis. *Clin Immunol* 2008, 128:172-180.
 28. Kelso ML, Elliott BR, Haverland NA, Mosley RL, Gendelman HE: Granulocyte-macrophage colony stimulating factor exerts protective and immunomodulatory effects in cortical trauma. *J Neuroimmunol* 2015, 278:162-173.
 29. Sugiyama Y, Yagita Y, Oyama N, et al. Granulocyte colony-stimulating factor enhances arteriogenesis and ameliorates cerebral damage in a mouse model of ischemic stroke. *Stroke* 2011, 42:770-775.
 30. Hotta M, Yoshimura H, Satake A, Tsubokura Y, Ito T, Nomura S: GM-CSF therapy inhibits chronic graft-versus-host disease via expansion of regulatory T cells. *Eur J Immunol* 2019, 49:179-191.
 31. Sheng JR, Muthusamy T, Prabhakar BS, Meriggioli MN: GM-CSF-induced regulatory T cells selectively inhibit anti-acetylcholine receptor-specific immune responses in experimental myasthenia gravis. *J Neuroimmunol* 2011, 240-241:65-73.
 32. Schutt CR, Gendelman HE, Mosley RL: Tolerogenic bone marrow-derived dendritic cells induce neuroprotective regulatory T cells in a model of Parkinson's disease. *Mol Neurodegener* 2018, 13:26.
 33. Weinhage T, Dabritz J, Brockhausen A, et al. Granulocyte macrophage colony-stimulating factor-activated CD39(+)/CD73(+) murine monocytes modulate intestinal inflammation via induction of regulatory T cells. *Cell Mol Gastroenterol Hepatol* 2015, 1:433-449 e431.
 34. Potter H, Woodcock J, Boyd T, et al. Interim report of a phase 2 pilot safety and efficacy trial of GM-CSF/Leukine in mild-to-moderate Alzheimer's disease. *Alzheimer's & Dementia* 2017, 13:P1572.
 35. Lieschke GJ, Maher D, O'Connor M, et al.: Phase I study of intravenously administered bacterially synthesized granulocyte-macrophage colony-stimulating factor and comparison with subcutaneous administration. *Cancer Res* 1990, 50:606-614.
 36. Cebon JS, Bury RW, Lieschke GJ, Morstyn G: The effects of dose and route of administration on the pharmacokinetics of granulocyte-macrophage colony-stimulating factor. *Eur J Cancer* 1990, 26:1064-1069.
 37. Hovgaard D, Mortensen BT, Schifter S, Nissen NI: Clinical pharmacokinetic studies of a human haemopoietic growth factor, GM-CSF. *Eur J Clin Invest* 1992, 22:45-49.
 38. Korzenik JR, Dieckgraefe BK, Valentine JF, Hausman DF, Gilbert MJ, Sargramostim in Crohn's Disease Study G: sargramostim for active Crohn's disease. *N Engl J Med* 2005, 352:2193-2201.
 39. Stern AC, Jones TC: The side-effect profile of GM-CSF. *Infection* 1992, 20 Suppl 2:S124-127.
 40. Jackson-Lewis V, Przedborski S: Protocol for the MPTP mouse model of Parkinson's disease. *Nat Protoc* 2007, 2:141-151.
 41. Benner EJ, Mosley RL, Destache CJ, et al. Therapeutic immunization protects dopaminergic neurons in a mouse model of Parkinson's disease. *Proc Natl Acad Sci U S A* 2004, 101:9435-9440.
 42. Hartwig T, Zwicky P, Schreiner B, et al. Regulatory T cells restrain pathogenic T helper cells during skin inflammation. *Cell Rep* 2018, 25:3564-3572 e3564.
 43. Delmer A, Karmochkine M, Cadiou M, Gerhartz H, Zittoun R: Recurrent spleen enlargement during cyclic granulocyte-macrophage colony-stimulating factor therapy for myelodysplastic syndrome. *Am J Hematol* 1990, 34:73-74.
 44. Peters M, Schirmacher P, Goldschmitt J, et al. Extramedullary expansion of hematopoietic progenitor cells in interleukin (IL)-6-sIL-6R double transgenic mice. *J Exp Med* 1997, 185:755-766.
 45. Gowda S, Desai PB, Hull VV, Math AA, Vernekar SN, Kulkarni SS: A review on laboratory liver function tests. *Pan Afr Med J* 2009, 3:17.
 46. Busher JT: Serum albumin and globulin. In *Clinical methods: the history, physical, and laboratory examinations*. Edited by rd, Walker HK, Hall WD, Hurst JW. Boston; 1990
 47. Liu M, Zhao X, Ma Y, Zhou Y, Deng M, Ma Y: Transcription factor c-Maf is essential for IL-10 gene expression in B cells. *Scand J Immunol* 2018, 88:e12701.

48. Jankovic D, Kugler DG, Sher A: IL-10 production by CD4+ effector T cells: a mechanism for self-regulation. *Mucosal Immunol* 2010, 3:239-246.
49. Chaudhry A, Samstein RM, Treuting P, et al. Interleukin-10 signaling in regulatory T cells is required for suppression of Th17 cell-mediated inflammation. *Immunity* 2011, 34:566-578.
50. Malhotra N, Leyva-Castillo JM, Jadhav U, et al. ROR α -expressing T regulatory cells restrain allergic skin inflammation. *Sci Immunol* 2018, 3:21.
51. Li Z, Li D, Tsun A, Li B: FoxP3+ regulatory T cells and their functional regulation. *Cell Mol Immunol* 2015, 12:558-565.
52. Cipolletta D, Feuerer M, Li A, et al. PPAR- γ is a major driver of the accumulation and phenotype of adipose tissue Treg cells. *Nature* 2012, 486:549-553.
53. Hamaguchi M, Sakaguchi S: Regulatory T cells expressing PPAR- γ control inflammation in obesity. *Cell Metab* 2012, 16:4-6.
54. Schabitz WR, Kruger C, Pitzer C, et al. A neuroprotective function for the hematopoietic protein granulocyte-macrophage colony stimulating factor (GM-CSF). *J Cereb Blood Flow Metab* 2008, 28:29-43.
55. Huang X, Choi JK, Park SR, et al. GM-CSF inhibits apoptosis of neural cells via regulating the expression of apoptosis-related proteins. *Neurosci Res* 2007, 58:50-57.
56. Shultz SR, Tan XL, Wright DK, et al. Granulocyte-macrophage colony-stimulating factor is neuroprotective in experimental traumatic brain injury. *J Neurotrauma* 2014, 31:976-983.
57. Choudhury ME, Sugimoto K, Kubo M, et al. A cytokine mixture of GM-CSF and IL-3 that induces a neuroprotective phenotype of microglia leading to amelioration of (6-OHDA)-induced Parkinsonism of rats. *Brain Behav* 2011, 1:26-43.
58. Baek H, Ye M, Kang GH, et al.: Neuroprotective effects of CD4+ CD25+FoxP3+ regulatory T cells in a 3xTg-AD Alzheimer's disease model. *Oncotarget* 2016, 7:69347-69357.
59. Reynolds AD, Stone DK, Mosley RL, Gendelman HE: Nitrated α -synuclein-induced alterations in microglial immunity are regulated by CD4+ T cell subsets. *J Immunol* 2009, 182:4137-4149.
60. Kiyota T, Machhi J, Lu Y, et al. URM-099 facilitates amyloid-beta clearance in a murine model of Alzheimer's disease. *J Neuroinflammation* 2018, 15:137.
61. Przedborski S, Jackson-Lewis V: Mechanisms of MPTP toxicity. *Mov Disord* 1998, 13 Suppl 1:35-38.
62. Popovic B, Golemac M, Podlech J, et al. IL-33/ST2 pathway drives regulatory T-cell-dependent suppression of liver damage upon cytomegalovirus infection. *PLoS Pathog* 2017, 13:e1006345.
63. Du LX, Wang YQ, Hua GQ, Mi WL: IL-33/ST2 pathway as a rational therapeutic target for CNS diseases. *Neuroscience* 2018, 369:222-230.
64. Liu Q, Dwyer GK, Zhao Y, Li H, et al.: IL-33-mediated IL-13 secretion by ST2+ Tregs controls inflammation after lung injury. *JCI Insight* 2019, 4.
65. Reichenbach DK, Schwarze V, Matta BM, et al.: The IL-33/ST2 axis augments effector T-cell responses during acute GVHD. *Blood* 2015, 125:3183-3192.
66. Siede J, Frohlich A, Datsi A, et al. IL-33 receptor-expressing regulatory T cells are highly activated, Th2 biased and suppress CD4 T cell proliferation through IL-10 and TGF β release. *PLoS One* 2016, 11:e0161507.
67. Piao WH, Jee YH, Liu RL, et al. IL-21 modulates CD4+ CD25+ regulatory T-cell homeostasis in experimental autoimmune encephalomyelitis. *Scand J Immunol* 2008, 67:37-46.
68. Spolski R, Kim HP, Zhu W, Levy DE, Leonard WJ: IL-21 mediates suppressive effects via its induction of IL-10. *J Immunol* 2009, 182:2859-2867.
69. Liu T, Zhang L, Joo D, Sun SC: NF- κ B signaling in inflammation. *Signal Transduct Target Ther* 2017, 2.
70. Kuklina EM, Shirshov SV: Role of transcription factor NFAT in the immune response. *Biochemistry (Mosc)* 2001, 66:467-475.
71. Becskei A, Grusby MJ: Contribution of IL-12R mediated feedback loop to Th1 cell differentiation. *FEBS Lett* 2007, 581:5199-5206.
72. Martin E, Nathan C, Xie QW: Role of interferon regulatory factor 1 in induction of nitric oxide synthase. *J Exp Med* 1994, 180:977-984.
73. You K, Sun P, Yue Z, Li J, Xiong W, Wang J: NOR1 promotes hepatocellular carcinoma cell proliferation and migration through modulating the Notch signaling pathway. *Exp Cell Res* 2017, 352:375-381.

Publisher's Note Springer Nature remains neutral with regard to jurisdictional claims in published maps and institutional affiliations.

Affiliations

Katherine E. Olson¹ · Krista L. Namminga¹ · Aaron D. Schwab¹ · Mackenzie J. Thurston¹ · Yaman Lu¹ · Ashley Woods² · Lei Lei² · Weijun Shen² · Feng Wang³ · Sean B. Joseph² · Howard E. Gendelman^{1,4} · R. Lee Mosley^{1,4}

¹ Department of Pharmacology and Experimental Neuroscience, Center for Neurodegenerative Disorders, University of Nebraska Medical Center, Omaha, NE 68198, USA

² Calibr, a Division of Scripps Research, La Jolla, CA 92037, USA

³ Key Laboratory of Protein and Peptide Pharmaceuticals, Institute of Biophysics, Chinese Academy of Sciences, Beijing 100101, China

⁴ Department of Pharmacology and Experimental Neuroscience, University of Nebraska Medical Center, Omaha, NE 6898-5880, USA